Joint Photonic Reservoir Computing and Demultiplexing Using Parallelly Coupled Micro-Ring Resonators for Eight-Channel Intra-DCN Application

Mohammad Seifi Laleh, Sebastian Kühl, Annika Dochhan, Silas Oettinghaus, Stephan Pachnicke
Chair of Communications, Kiel University, Kiel, Germany, mohammad.seifi-laleh@tf.uni-kiel.de

Abstract— **We present a photonic reservoir computer based on cascaded add/drop micro-ring resonators, performing signal equalization and simultaneous demultiplexing in a short-reach 1.6 Tb/s WDM transmission. The photonic reservoir improves receiver sensitivity ~3 dB and outperforms DSP-based FFE, either by reducing BER or DSP complexity significantly in comparison.**

Keywords— Wavelength division multiplexing, reservoir computing, signal equalization, short reach transmission

I. INTRODUCTION

To obtain high bitrate intra-DCN connectivity at 1.6 Tb/s data rate, eight channel wavelength division multiplexing (WDM) transmission at 200 Gb/s/λ net line rate is a solution, resulting in a cost-effective short-reach communication system. Typically, O-band transmission based on intensity-modulation and direct-detection (IM/DD) using pulse amplitude modulation (PAM-4) and standard single-mode fiber (SSMF) is employed [1]. The very high symbol rate requires use of digital signal processing (DSP) based equalizers. Further scaling of the data rate can be achieved by using higher symbol rates and modulation order, or additional WDM lanes. The maximum achievable data rate is bound by the received optical power (ROP), accumulated chromatic dispersion (CD), bandwidth limitations (BWL), multi-path interference (MPI) and fiber nonlinearities, calling for complex equalizers [2].

It has been shown that a reservoir computer (RC) as a type of a recurrent neural network (RNN) can be used for photonic signal equalization [3-5]. A photonic RC reduces the algorithmic DSP complexity by shifting computation partially into the optical domain. It only requires training of a linear output layer, while the hidden layers' weights remain static. This approach has advantages in terms of easier training compared to RNNs and makes realization in the form of micro-ring resonators (MRRs) on photonic integrated circuit (PIC) possible. In [6], we have shown the integrated demultiplexer and reservoir computer architecture for a two channel WDM transmission, which however still requires an additional filtering/demux stage in case of eight channel WDM to provide four groups of two channels. Here, we present for the first time to our knowledge a photonic RC based on eight stages of parallelly coupled MRRs for joint optical signal equalization and demultiplexing in an eight channel 112 GBd PAM-4 1.6 Tbit/s short-reach WDM IM/DD transmission, which allows to omit an additional demultiplexer at the receiver (Rx). In our approach the MRRs work as a photonic RC for any specified channel leading to an improved bit error ratio (BER) compared to an equivalently complex feed-forward equalizer (FFE) based DSP. We show that the proposed configuration can equalize eight-channel signals with different amounts of accumulated CD and different ROPs. We employed a resonance wavelength shift mechanism to overcome challenges of designing optimum parameters of the RC, enabling low complexity and high bitrate multi-channel equalization for next generation short-reach WDM transmission systems.

II. SYSTEM SETUP

The channel plan of the WDM transmission system and the zero-dispersion wavelength (ZDW) are selected based on design considerations for 1.6 Tbit/s intra-DCN systems [7]. The 112 GBd PAM-4 transmission system consisting of eight WDM channels, up to 5 km reach of SSMF, demultiplexer and FFE-based DSP is shown in Fig. 1a representing a baseline. Alternatively, for the same transmission system a PIC is inserted at the Rx side acting as both a demultiplexer and RC-based equalizer (Fig. 1b). The eight wavelengths from 1291.1 nm to 1323 nm correspond to the LDWM-8 channels in the O-band, spaced on an 800 GHz frequency grid. The edge channels correspond to the wavelengths with the highest distance from the ZDW and therefore highest accumulated CD.

The optical signals are generated by electro-absorption modulated lasers (EAM) with a linewidth enhancement factor $\alpha_c = -1$ and an optical launch power of 0 dBm/ch into the fiber. The signal is impaired by CD, modulator chirp, BWLs of the individual components, and noise, while nonlinear transmission effects, polarization mode dispersion and MPI are not considered in the numeric simulation. A pseudo-random binary sequence (PRBS) with 2^{20} bits is used to generate a sufficient number of bits to estimate a BER below HD-FEC (3.8×10^{-3}) and KP4 (2.2×10^{-4}) thresholds. The mapping corresponds to 112 GBd PAM-4 non-return-to-zero waveforms, which are shaped by a raised cosine function with the roll-off factor of 0.05. The transmit side BWL is modelled by a second-order Butterworth filter with cut-off frequency of 44.8 GHz (40% of baudrate). The SSMF is modelled using the non-linear Schrödinger equation with a dispersion slope of 0.09 ps/nm^2/km and ZDW 1312 nm. For comparability between the equalization schemes, the ROP is matched for both equalization schemes before the photodiode (PD), which considers shot noise, dark current and thermal noise. For both, FFE and RC the sampling rate (224 GSa/s) for the analog-to-digital conversion and normalization are identical. The RC readout is based on ridge regression with a regularization factor $\alpha_R = 1$ which is trained by singular value decomposition. Both RC and FFE use 4,096 training symbols, while the FFE taps and readout coefficients are kept frozen after training.

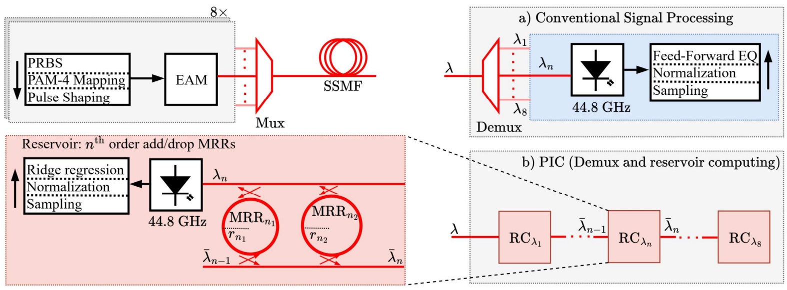

Fig. 1. Simulated IM/DD transmission setup for an **8** channel WDM system and signal equalization using a) FFE based signal processing with separate demultiplexing, b) MRR-based reservoir computing with integrated demultiplexer, λ_n: dropped signal, $\bar{\boldsymbol{\lambda}}_{\boldsymbol{n}}$: through passed signal, $\bar{\boldsymbol{\lambda}}_{\boldsymbol{n-1}}$: input signal, EAM: electro-absorption modulated laser, PAM: pulse amplitude modulation, PRBS: pseudo-random binary sequence, SSMF: standard single-mode fiber.

The reservoir structure contains eight stages (one per WDM channel), of which each one is comprised of two parallelly coupled add/drop MRRs as shown in Fig.1b. These 16 MRRs are arranged between a common input bus waveguide and eight separated drop bus waveguides. Here all straight and curved waveguides are silicon-on-insulator (SOI) with dimensions of 220 × 450 nm. Each pair of resonators selects one specified channel wavelength, resulting in an RC with integrated demultiplexer. Increasing the number of MRRs provides more effective optical paths (EOPs), affecting the RC's memory capacity and phase shift, but fabrication constraints, chip footprint, propagation losses, coupling gaps, and resonance detuning limit implementations to a few cascaded MRRs. Thus, we use two MRRs per stage, forming two parallel rings with a feedback loop, increasing EOP.

In each stage, the second resonator is forming an optical feedback path between the throughput and add ports of the previous resonator. Efficient feedback is achieved at each stage, provided that wavelength detuning of the first resonator is non-zero. Thus, the input port of the second resonator contains signals from the input and throughput ports of the first MRR. In addition, the detuning of the second MRR should be in the range of a few picometer to keep the resonator in a pure resonance mode and to form an optical feedback path with low leakage. The first RC gets the input signal (λ), containing all wavelengths. So, the second one gets $\bar{\boldsymbol{\lambda}}_{\boldsymbol{i}}$ which has only 7 wavelengths, excluding the one that is filtered out in the first stage. Thus, the last RC input is only $\bar{\boldsymbol{\lambda}}_8$ that is detected in the last drop port. Although each pair of MRRs is designed to select the specified wavelength, it potentially can cause unwanted resonances overlapping with neighbouring channels. Before the photodiodes, all signals are set to an identical power by an optical attenuator. This allows the BER to be compared at the same ROP.

Furthermore, by keeping the center-to-center distance between two subsequent MRRs greater than half of the circumference of the previous resonator, mutual coupling between the cascaded resonators is prevented [8]. The radii, gaps between straight and curved waveguides and waveguide dimensions of the fabricated chips may differ from designed parameters due to the fabrication tolerances of the CMOS foundry. Besides, ambient temperature variation and the excitation of the ring in the on-resonance mode might change the temperature of the PIC which affect the performance of the RC by shifting the resonance wavelengths. In practical cases it would not necessarily imply degradation of the overall performance of the RC, as they behave as random weights within the reservoir. However, it is feasible to compensate the deviations using electronic micro-heaters in silicon photonics technology [9] while post-fabrication tuning of the coupling coefficient can be done by using interferometric couplers. In practice, thermal heaters can provide resonance detuning of MRRs [10]. In this study, the coupled-mode theory (CMT) equations are used to derive ordinary differential equations for the intra-cavity field, the free carrier density and the rate of change of the temperature of the nonlinear MRR in each stage follow the method being explained in [3, 11-13]. In this research, first we design MRRs' radii, then the grid search is used to find optimum coupling coefficients and wavelength detuning factors to achieve minimum BER at a specified ROP.

III. Results

The RC parameters are listed in Tab. 1. The MRR radii in each stage are designed to select the desired WDM channel. Commonly, reservoirs are characterized by their memory capacity, and input separability [14]. The upper bound of the memory capacity might be limited by the accumulated CD, but a method to parametrize the RC based on the cascaded MRRs for signal equalization in the mentioned transmission scenario is unknown. Therefore, the number of cascaded MRRs, the length between two subsequent rings, coupling gaps, and wavelength detuning are directly optimized by grid search to minimize the BER for a fixed ROP of −8 dBm and 2 km of reach using 20 multiply-accumulate (MAC) operations per symbol.

Table 1. RC parameters for the MRR radius r_i and the wavelength detuning $\Delta\lambda_i$ is wavelength detuning of the i-th MRR.

n	λ_n [nm]	r_{n1} [µm]	r_{n2} [µm]	$\Delta\lambda_{n1}$ [µm]	$\Delta\lambda_{n2}$ [pm]
1	1323.00	16.2	16.2	-220	-10
2	1318.35	10.6	10.6	200	10
3	1313.73	20	13.8	-200	-30
4	1309.14	20	15.5	80	-40
5	1304.58	52	48.7	80	50
6	1300.05	30	27.3	100	-60
7	1295.56	35	32.8	160	10
8	1291.10	24.7	20	-220	50

The comparison in terms of BER of RC and FFE-based equalization for different reaches of the edge channel which experiences the most CD penalty (due to chirp effects) at λ_1 = 1323 nm is shown in Fig. 2. Both cascaded MRRs and FFE use 50 taps and are therefore directly comparable in terms of the DSP complexity after detection. Here, the required ROP to reach the HD-FEC threshold improved by ~2.7 dB, resulting in a BER reduction from 7.6 × 10^{-3} to 4 × 10^{-5} for 5 km fiber length at -10 dBm. System performance for all eight channels and a transmission length of 2 km is shown in Fig. 3. The RC reduces the BER compared to FFE for all investigated wavelengths, independent of the ROP. For lower ROP values, the BER is decreased for λ_8 = 1291.1 nm from 1.8× 10^{-2} using FFE to the KP4 threshold at -11.7 dBm using the RC. The RC performance improvement shown in Figs. 2 and 3 can also enhance the reach of the transmission system or alternatively allows less complex DSP. To investigate the latter case, the required number of MAC operations per received symbol at -8 dBm to reach a BER below the KP4 threshold is evaluated for varying accumulated dispersion values or the equivalent fiber length.

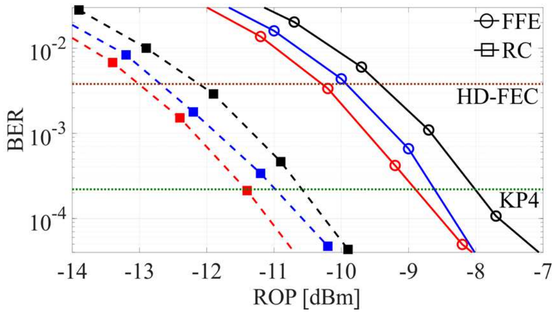

Fig. 2. Comparison of BER vs. ROP when either RC or FFE are used for signal equalization considering the most impaired edge channels (λ_1 = 1323 nm) in the 8 x 224 Gb/s scenario over a SSMF with a length of 500 m (red), 2 km (blue) and 5 km. (black).

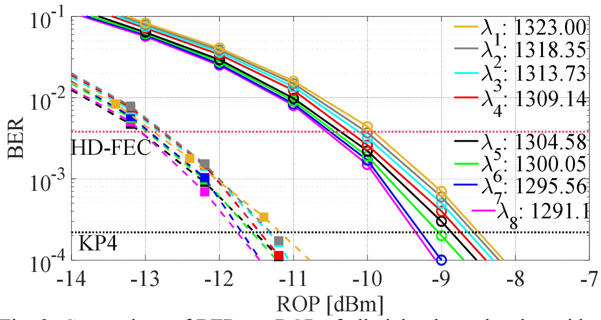

Fig. 3. Comparison of BER vs. ROP of all eight channels when either FFE (solid lines, circle markers) and RC (dash lines, square markers) are used for signal equalization, transmission over 2km SSMF.

Results are depicted in Fig. 4. In this case, the edge channels have been considered at 1323nm and 1291.1nm respectively. Here we use the number of MAC operations instead of the number of taps in the FFE to directly compare the complexity of the DSP with the RC [3]. The optimized RC-based equalization reduces the required number of MAC operations for an accumulated CD greater than 8 ps/nm compared to an FFE. With 38 MAC operations per symbol for λ_1 and 21 for λ_8, the RC is able to equalize the signal at 10 ps/nm of accumulated dispersion, where the FFE based DSP require 68 and 47 MAC operations for identical performance for λ_1 and λ_8, respectively.

IV. Conclusions

A photonic integrated circuit based on add/drop micro-ring resonators has been numerically investigated for its signal equalization performance of an eight-channel 112 Gbaud PAM-4 WDM short reach transmission system. The proposed scheme acts simultaneously as an integrated demultiplexer so that an otherwise required demultiplexer at the Rx can be omitted. The proposed scheme reduces the ROP requirement by 2.7 dB compared to FFE based DSP with identical complexity. By adding more cascaded add/drop stages, the scheme is expected to support higher numbers of WDM channels, enabling simultaneous equalization and demultiplexing in a 16-channel 3.2 Tb/s IM/DD transmission system in the future.

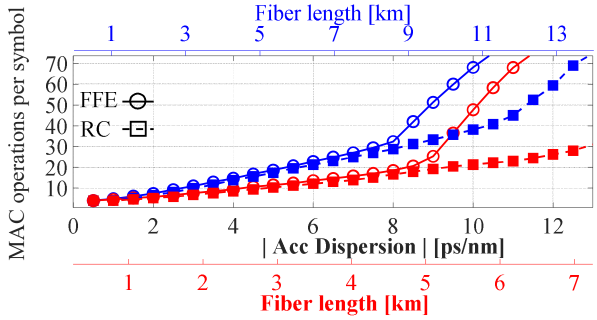

Fig. 4. Required number of MAC per received symbol at -8 dBm ROP for a BER below the KP4 by using FFE and RC equalizers at λ_1 = 1323 nm (blue) and λ_8 = 1291.1 nm (red).

Acknowledgment

The authors acknowledge the financial support by Deutsche Forschungsgemeinschaft (DFG, German Research Foundation), project number 498410117 and by the German Ministry of Research, Technology and Space (BMFTR) in the framework of the project 6G-RIC 16KISK021.

References

[1] X. Zhou, C. F. Lam, R. Urata, and H. Liu, ''State-of-the-Art 800G/1.6T Datacom Interconnects and Outlook for 3.2T'', Optical Fiber Communication Conference, pp. W3D-1, 2023.

[2] D. Che and X. Chen, "Modulation Format and Digital Signal Processing for IM-DD Optics at Post-200G Era", J. Lightwave Technol., pp. 588-605, 2024.

[3] S. Kühl, M. S. Laleh, A. Mataji-Kojouri, S. Oettinghaus, K. Jamshidi, and S. Pachnicke, "Cascaded Micro-Ring Resonator based Reservoir Computing for Optical Equalization of PAM-4 Short Reach Signals", J. Lightwave Technol, pp. 7285-7292, 2025.

[4] F. Da Ros, S. M. Ranzini, H. Bülow, and D. Zibar, "Reservoir-computing based equalization with optical pre-processing for short-reach optical transmission", IEEE Journal of Selected Topics in Quantum Electronics, pp.1-12, 2020.

[5] Y. Dong, et al, "Equalization of Short-Reach IMDD Transmission with Enhanced Reservoir Computing", J. Lightwave Technol, pp. 1212-1221 , 2024.

[6] M. S. Laleh, S. Kühl, S. Oettinghaus, and S. Pachnicke, "Micro-Ring Resonator Based Reservoir Computer for Short-Reach WDM Signal Equalization", European Conference on Optical Communications (ECOC), 2025.

[7] A.A. Juarez, Y. Zhu, X. Chen, and M. J. Li, "Design Considerations for 1.6 Tbit/s Data Center Interconnects: Evaluating IM/DD and Coherent Transmission over O-Band Transmission Window", Photonics, p. 1179, 2024.

[8] R. Grover, et al, "Parallel-cascaded semiconductor microring resonators for high-order and wide-FSR filters", J. Lightwave Technol, p. 872, 2002.

[9] Y. Xie et al., "Thermally-reconfigurable silicon photonic devices and circuits," IEEE J. Sel. Topics Quantum Electron., pp. 1-20, 2020.

[10] K. Padmaraju, J. Chan, L. Chen, M. Lipson, and K. Bergman, "Thermal stabilization of a microring modulator using feedback control," Opt. Exp., pp.27999-28008, 2012.

[11] V. Van, Optical Microring Resonators: Theory, Techniques, and Applications, 1st ed., CRC Press, 2016.

[12] B. E. Little, S. T. Chu, H. A. Haus, J. Foresi, and J.- P. Laine, "Microring resonator channel dropping filters", J. Lightwave Technol, pp. 998– 1005, 1997.

[13] G. Donati, C. R. Mirasso, M. Mancinelli, L. Pavesi, and A. Argyris, "Microring resonators with external optical feedback for time delay reservoir computing", Optics Express, pp. 522–537, 2022.

[14] K. Nakajima and I. Fischer, Reservoir Computing: Theory, Physical Implementations, and Applications. Cham, Switzerland: Springer, 2021.